

Direct radiance validation of IASI - results from JAIVEx

S. M. Newman, F. Hilton and J. P. Taylor

Met Office, FitzRoy Road, Exeter EX1 3PB, UK

A. D. Collard

European Centre for Medium-Range Weather Forecasts, Reading RG2 9AX, UK

W. L. Smith

Hampton University, Hampton, Virginia 23668

A. Larar

NASA Langley Research Center, Hampton, Virginia 23681

The Joint Airborne IASI Validation Experiment (JAIVEx) was based in Houston, Texas during April and May 2007. This dataset, combining collocated hyperspectral infrared radiance measurements and in situ sampling of the atmospheric state, has been used to validate IASI radiances and identify sources of error in the radiative transfer modelling. The calibration accuracy of IASI radiances is shown to be valid to within 0.2 – 0.3 K. Characterisation of surface emissivity and skin temperature is shown to be important for accurate radiative transfer modelling of IASI spectra over land. This dataset is available to the wider community for investigations into the exploitation of IASI data in numerical weather prediction.

1. Description of the campaign

The methodology underpinning airborne research studies into satellite calibration and validation is to characterise rigorously both the absolute upwelling atmospheric radiance and the state of the atmosphere (in particular fields of temperature and humidity). Temporal and spatial collocation of these measurements is important to minimise representivity errors. Airborne hyperspectral sounders have been demonstrated to be of particular benefit in constraining calibration errors and developing algorithms for retrieval of atmospheric state vectors (Taylor et al., 2008; Tobin et al., 2006).

The Joint Airborne IASI Validation Experiment (JAIVEx) brought together the UK Facility for Airborne Atmospheric Measurements (FAAM) BAe 146 aircraft and the NASA WB-57 high altitude research aircraft. Both are comprehensively instrumented airborne research platforms, well suited to satellite cal/val exercises of this kind. Flights of the two aircraft were coordinated with overpasses of IASI on the MetOp-A satellite. The campaign was based in Houston, Texas during April and May 2007, with sorties conducted over ocean (Gulf of Mexico) and over land (ARM Southern Great Plains facility, Oklahoma). This dataset can be exploited to test the absolute radiative accuracy of IASI and hyperspectral retrieval algorithms over different surfaces.

The FAAM aircraft instrument capabilities include:

- Airborne Research Interferometer Evaluation System (ARIES) measuring upwelling and downwelling infrared radiances at 1 cm^{-1} spectral resolution;
- Heimann broadband infrared radiometer for mapping surface temperatures;
- AVAPS dropsonde system, allowing profiles of temperature and humidity below the aircraft to be sampled at high spatial resolution;
- Onboard temperature and humidity probes for measuring in situ atmospheric conditions, and aerosol and cloud probes for measuring particulates;
- Onboard chemistry probes for measuring in situ atmospheric concentrations of trace gases such as ozone and carbon monoxide.

The WB-57 aircraft carries two state-of-the art interferometers:

- Scanning High-resolution Interferometer Sounder (S-HIS) measuring upwelling and downwelling infrared radiances at 1 cm^{-1} spectral resolution;
- National Polar-orbiting Operational Environmental Satellite System (NPOESS) Airborne Sounder Testbed – Interferometer (NAST-I) measuring upwelling radiances at 0.5 cm^{-1} spectral resolution (comparable to IASI).

Both of these interferometers are scanning cross-track, i.e. measure a swath below the aircraft in a similar way to IASI on MetOp. For flights over the Oklahoma ARM site there was additional profile information through the launch of radiosondes and ground-based lidar and interferometer measurements.

In the case studies described here only measurements within the same geographic area and small time window have been considered, to give maximum confidence that all measurements relate to the same atmospheric airmass. Exclusively clear sky fields of view for radiometric measurements have been analysed, as determined from onboard observations and MetOp AVHRR imagery.

2. Line-by-line simulations

Atmospheric profiles for input to a line-by-line radiative transfer code, representative of the observed radiances, were constructed in the following way:

1. The nearest collocated dropsonde profile was used for temperature and humidity below the FAAM 146 altitude (typically around 10 km);
2. Trace gas profiles for ozone and carbon monoxide were derived for this lower atmosphere range from in situ aircraft probes;

3. In the absence of closely coincident radiosonde observations, temperature and humidity for the upper atmosphere (above around 10 km) were derived from operational NWP model fields. Fields were available from both the Met Office and ECMWF global model forecast (run from the closest previous analysis). Ozone was available as a variable parameter from the ECMWF model.
4. The surface skin temperature was derived from Heimann radiometer measurements, coupled with spot retrievals of temperature and emissivity using ARIES hyperspectral radiances.

GENLN2 (Edwards, 1992) was used as the line-by-line code. Recent updates to spectroscopic parameters (HITRAN 2004) and the water vapour continuum (MT_CKD_1.0) were implemented in the simulations.

3. Gulf of Mexico case study 30 April 2007

A coordinated BAe 146 and WB-57 flight on 30 April 2007 was conducted over the Gulf of Mexico, with a coincident MetOp overpass at 1529 UTC. Figure 1 shows that the south-western portion of the flight track was clear of cloud (confirmed by onboard observations), and the case study fields of view (FOVs) have been confined to this geographic area.

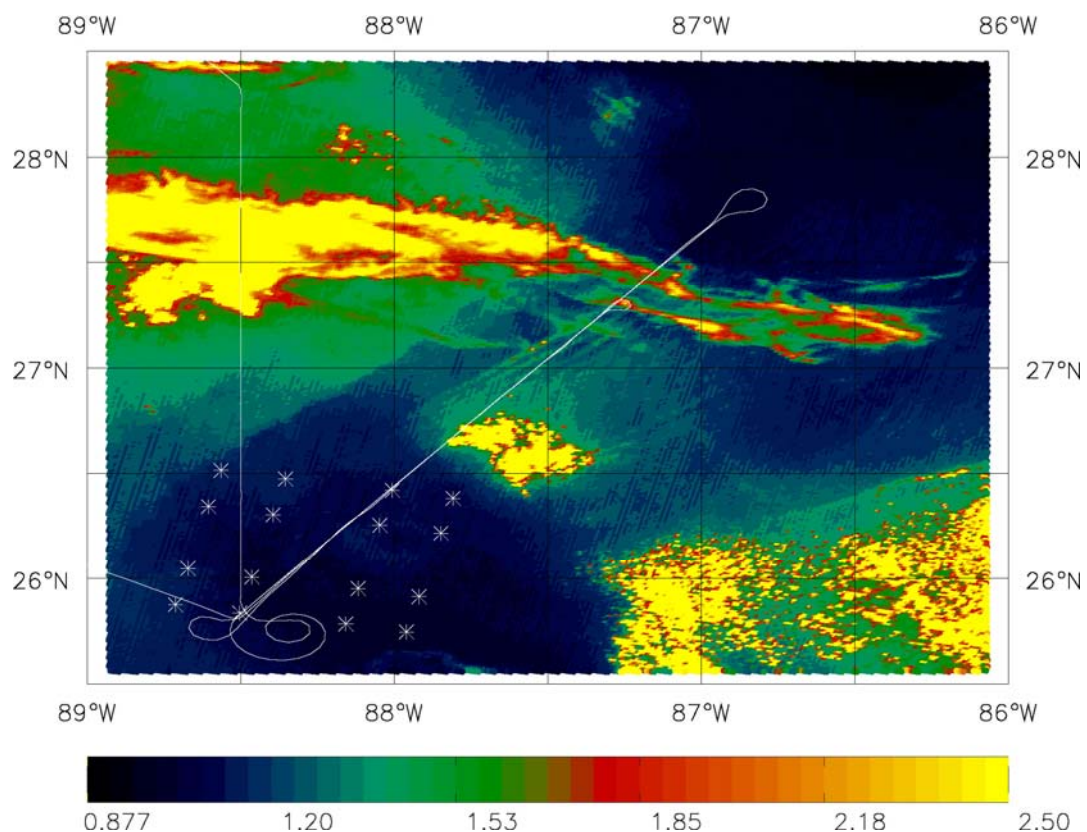


Figure 1: AVHRR channel 1 image (580-680 nm) from MetOp pass on 30 April 2007, overlaid with FAAM BAe 146 flight track and (white asterisks) selected clear IASI FOVs. The brightest parts of the AVHRR image show the presence of clouds due to solar reflection.

The FAAM BAe 146 launched several dropsondes in close time and space coincidence with the MetOp overpass. Figure 2 shows collocation of IASI and ARIES footprints in the clear air region together with four dropsonde profiles (all launched between 1519 and 1527 UTC, i.e. all were in the air during the overpass).

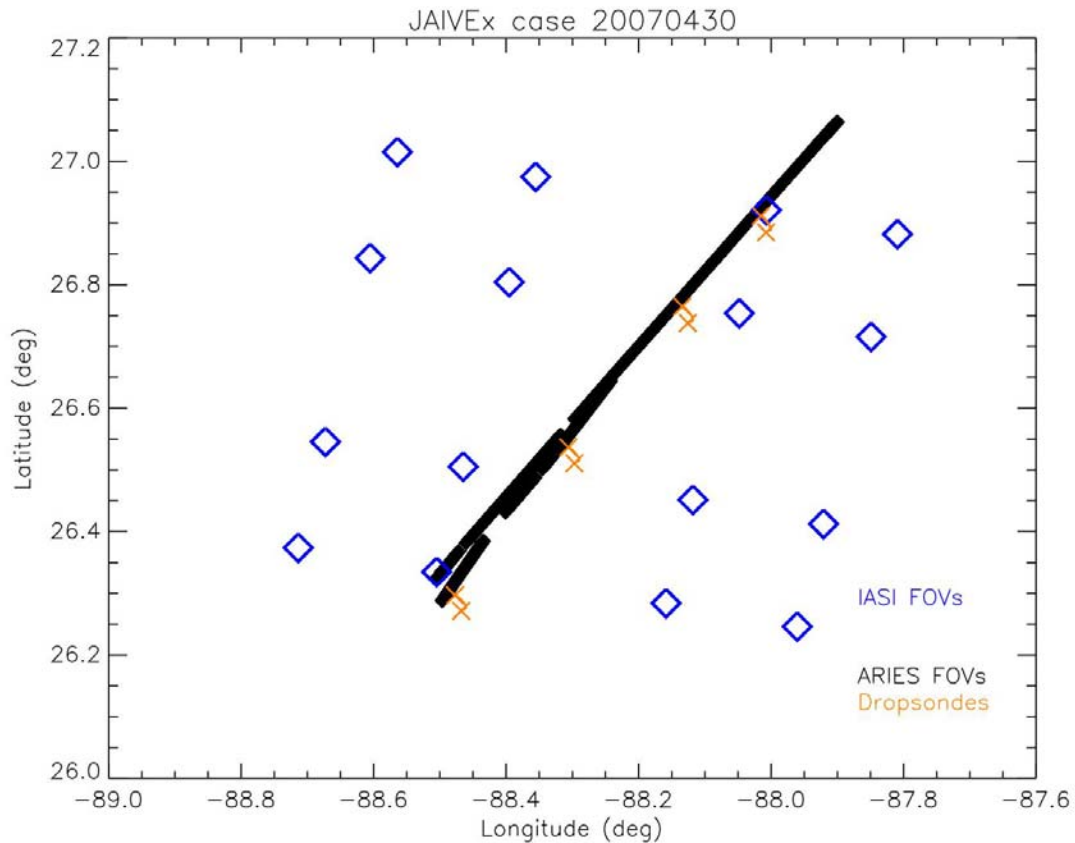


Figure 2: Collocation of observations during the measurement period. The diamond symbols denote (the centres of) individual instrument footprints on the ground, while crosses show the launch and splash coordinates of dropsondes, see legend.

Having carefully selected clear sky observations and collocated profile measurements, GENLN2 simulations were run for each of the four profiles (topped up with model fields); each interferometer field of view (FOV) was then matched to the nearest profile/simulation, and observed – calculated residuals computed. The average residuals are plotted in Figure 3 for the longwave spectral region. There are a number of points to note:

1. Due to the different altitudes of ARIES (around 10 km) and IASI (on MetOp) only IASI is sensitive to the upper atmosphere. There are therefore significant differences in the average spectra, particularly in bands sensitive to CO₂ and ozone.
2. The residuals generally lie within the ± 1 K level. Exceptions to this include the region above 1200 cm⁻¹ where the spectra are sensitive to methane (not measured during the campaign) and for IASI in the ozone band 1000-1100 cm⁻¹ which relies on

ozone concentrations from NWP models. The Met Office fields do not include variable ozone, hence climatological values have been used.

3. Apart from the ozone band, the Met Office and ECMWF fields used to “top-up” the tropospheric profiles derived from dropsondes give very similar results in the residuals plot for IASI in this spectral region.
4. Excluding the ozone band, the residuals in the 800-1200 cm^{-1} atmospheric window (sensitive mainly to sea surface emission and tropospheric water vapour continuum) are very small, on average -0.2 K.
5. The window region residuals for ARIES and IASI differ by less than 0.1 K, giving confidence in the absolute calibration accuracy.
6. Larger residual errors in the modelling of IASI data are found in other spectral regions, e.g. the strong water vapour band around 1400-1800 cm^{-1} . The reasons for this, related to the accuracy of model field data for the upper atmosphere, are discussed in detail in Newman et al., 2008.

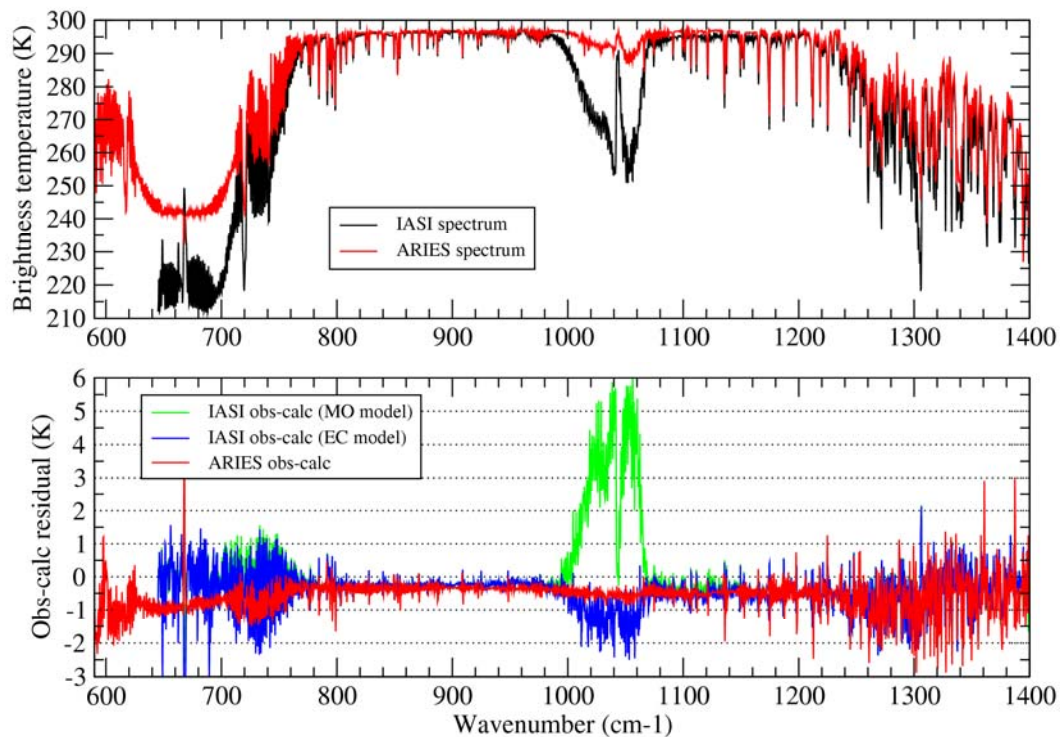


Figure 3: (Upper panel) IASI and ARIES clear-sky upwelling brightness temperature spectra recorded on 30 April 2007. (Lower panel) residual differences (observed – calculated GENLN2 spectrum) for both Met Office and ECMWF upper atmosphere fields, see legend.

The good level of agreement between observed and calculated radiances in Figure 3 can be attributed to a well constrained atmospheric profile and surface characteristics coupled with good calibration performance of the interferometers. It remains to test whether the results are sensitive to the line-by-line code used. Figure 4 compares the GENLN2 with results generated

with the LBLRTM code (Clough, 2005). LBLRTM contains more recent updates to some key spectroscopic parameters, particularly CO₂ line mixing. Figure 4 appears to show that LBLRTM is more successful than GENLN2 at reducing the size of residuals in the CO₂ band between 700-770 cm⁻¹. Other parts of the spectrum such as weak water vapour lines above 800 cm⁻¹ are much less affected (similar HITRAN line parameters were used in both codes). In the remainder of this paper the GENLN2 code has been used for simulations; Figure 4 suggests that the performance of this code is sufficient for drawing conclusions about radiometric accuracy, e.g. in the atmospheric window region.

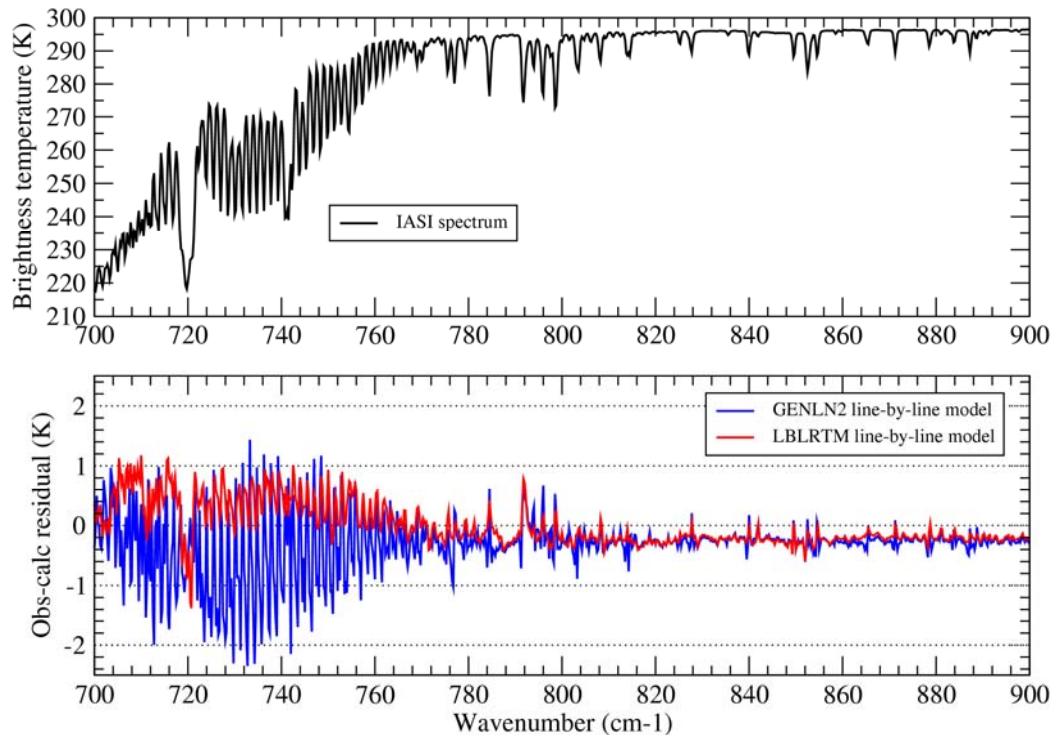


Figure 4: (Upper panel) IASI clear-sky upwelling brightness temperature spectrum for 30 April 2007. (Lower panel) residual differences (observed – calculated) for GENLN2 and LBLRTM (see legend) using ECMWF reference profile for the upper atmosphere.

4. Oklahoma case study 19 April 2007

A night-time flight was conducted on 19 April 2007 over the Oklahoma ARM CART site, with a coincident MetOp overpass at 0335 UTC. A north-south flight track was followed (Figure 5), and all available observations indicated that the atmosphere was clear of cloud at all levels. As in the previous case study, coincident interferometer and profile measurements were selected to obtain a self-consistent dataset for validation. Figure 6 summarises the observations for this case, with three dropsondes launched between 0320 and 0333 UTC. A radiosonde ascent from the ARM site at 0541 UTC was also available for independent profile information, albeit separated from the other measurements by two hours.

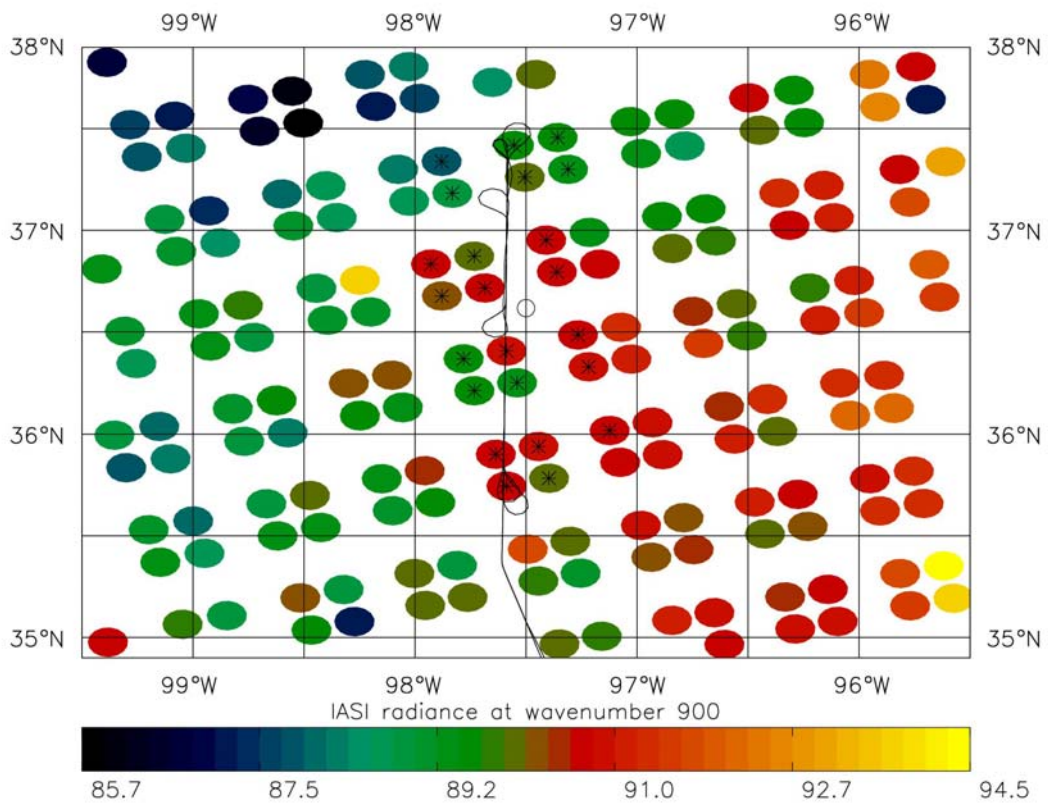


Figure 5: MetOp IASI radiances at channel 900 cm⁻¹ overlaid with FAAM BAe 146 flight track and (black asterisks) selected clear IASI FOVs. The position of the ARM CART site central facility is shown as the open circle. The variations in radiances are due to surface temperature and emissivity differences between FOVs.

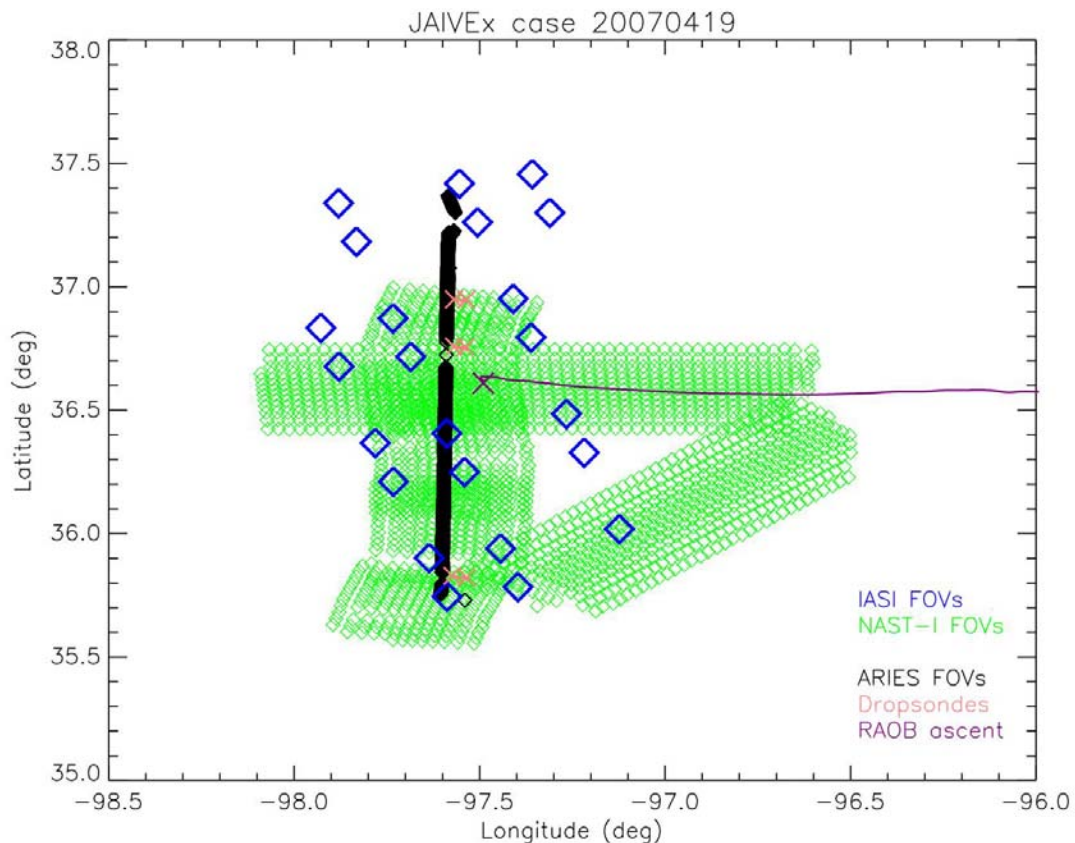


Figure 6: Collocation of observations during the measurement period. The diamond symbols denote (the centres of) individual instrument footprints on the ground, while crosses show the launch and terminating coordinates of dropsondes and radiosonde, see legend.

The FAAM BAe 146 completed two runs at 1 km altitude either side of high level (8-9 km) measurements to coincide with the MetOp overpass. These low level runs are invaluable for retrieval of surface properties to be used as boundary conditions for line-by-line simulations. The methodology used to retrieve surface skin temperatures and spectral emissivity from ARIES observations is described in detail in Newman et al. (2005).

Briefly, a combination of upwelling and downwelling ARIES spectra are used to differentiate between the spectrally structured downwelling radiance and (assumed) spectrally smooth surface emission. The fraction of downwelling radiance reflected at the surface (and thereby present in the upwelling radiance) is retrieved over spectral bands in the 800-1200 cm^{-1} region. This gives a coarse-resolution emissivity spectrum and simultaneously an estimate of surface skin temperature for each band. The average retrieved skin temperature is then used to derive an emissivity spectrum at full ARIES resolution.

Figure 7 shows the results of emissivity retrievals from the low level runs over the atmospheric window region. Note that principal component noise reduction has been applied to the ARIES radiances to facilitate the retrieval. There is a very broad spread of spectra, indicative of a mix of surface types in the Oklahoma region around the ARM site (largely arable land, a mix of vegetation and bare soil). The shape of the emissivity spectra with the lowest values, with an emissivity minimum around 1100 cm^{-1} , is characteristic of a

contribution by minerals in soil (R. Knuteson, private communication). Conversely, the ARIES footprints with a high fraction of vegetation exhibit a spectrally flat emissivity with values close to 1.0.

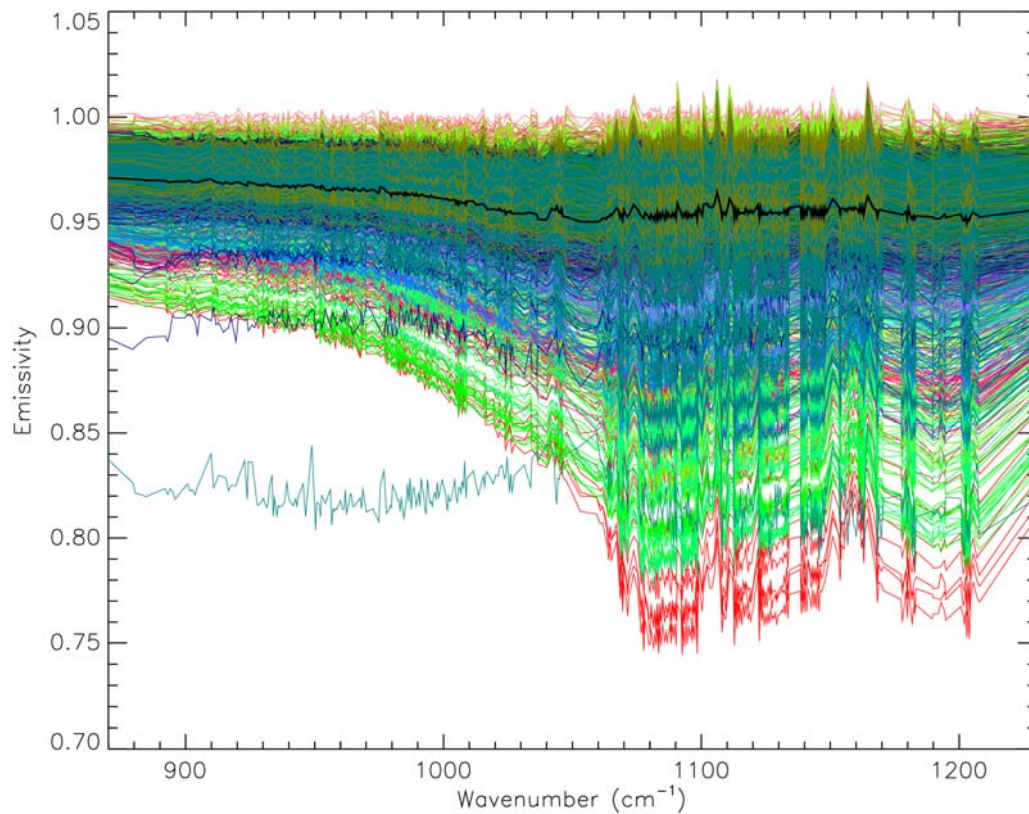


Figure 7: Individual emissivity retrievals from 4222 upwelling ARIES radiance spectra. The superimposed black line gives the average emissivity over this set. The outliers with low emissivity values around 900 cm^{-1} are believed to be real, consistent with artificial structures and buildings seen in the FAAM 146 downward-facing video footage.

The $800\text{-}1200\text{ cm}^{-1}$ region is best suited to emissivity retrieval due to a combination of high instrument signal-to-noise and high atmospheric transmittance. It is possible also to retrieve emissivity in other spectral regions, though with noisier results. Figure 8 shows the average emissivity retrieved from the ARIES low level data, including regions beyond 2000 cm^{-1} . There is a signal for a lower emissivity at 2500 cm^{-1} than at 1200 cm^{-1} .

Retrievals of surface skin temperature accompany those of emissivity (see Figure 9). There is a trend of decreasing temperature during the night, plausibly due to the effects of radiative cooling in clear sky conditions. In order to arrive at an average surface temperature value to be used in line-by-line simulations of interferometer radiances at the MetOp overpass time, the temperatures have been interpolated assuming a linear trend. This gives a representative surface skin temperature of 284.7 K . It should be noted that the standard deviation of the retrievals during each run is approximately 1.5 K ; this may well be due to real variations in surface temperature, but underlines the uncertainties in this retrieved parameter.

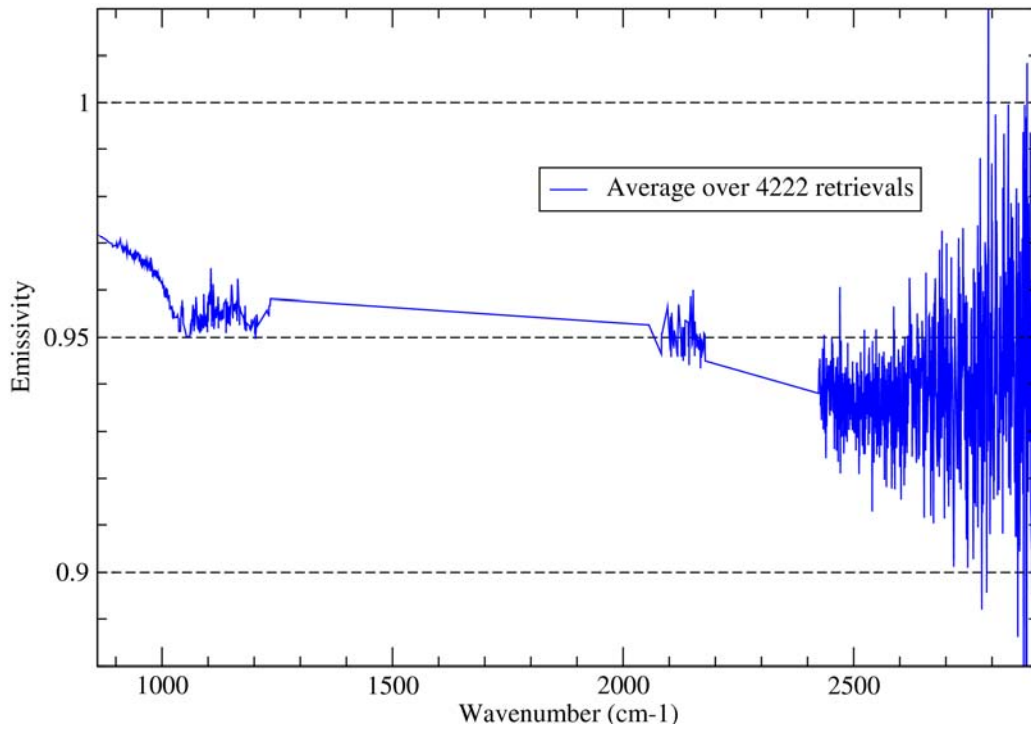


Figure 8: Average emissivity retrieval from 4222 upwelling ARIES radiances, covering spectral regions with sufficiently high atmospheric transmittance for retrieval.

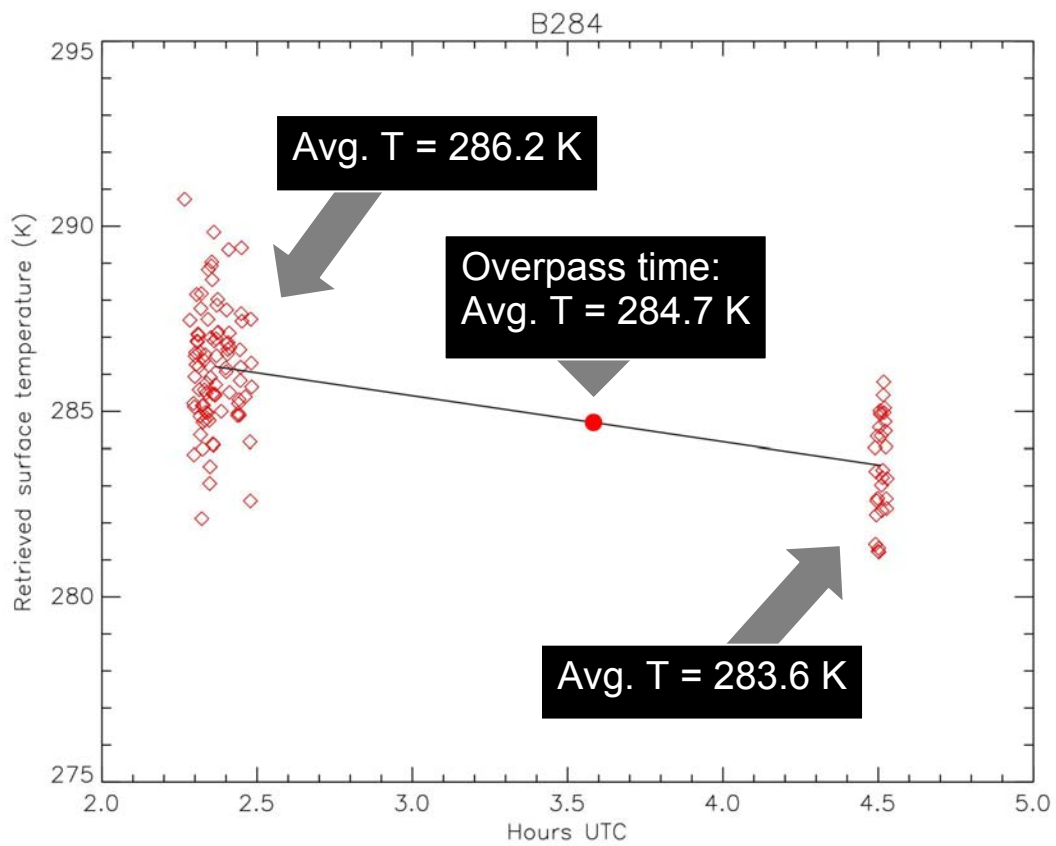


Figure 9: Retrieved surface temperature from ARIES data for 19 April 2007 case. Data for the two low level runs are interpolated to the overpass time of 0335 UTC.

Having characterised the land surface properties for this case study, line-by-line simulations have been run for the selected FOVs in a similar way as in Section 3. Figure 10 displays the average residuals over all FOVs for the longwave spectral region. The inclusion of the retrieved surface temperature and emissivity in the simulations is shown to restrict the obs – calc residuals to within ± 1 K over much of the atmospheric window.

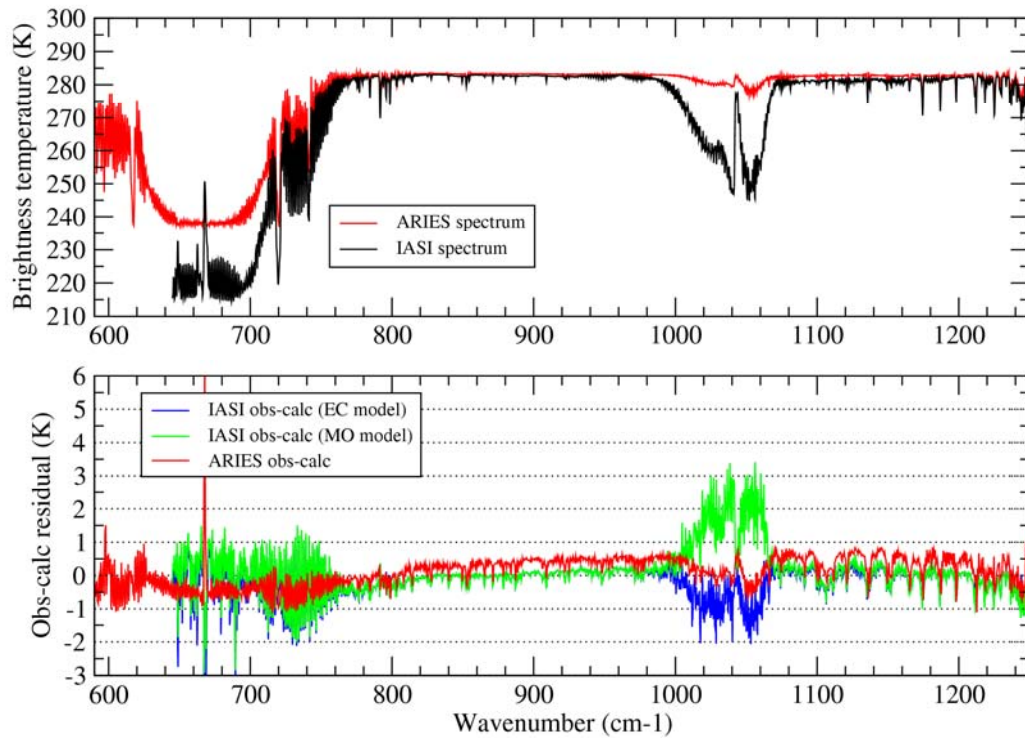


Figure 10: (Upper panel) IASI and ARIES clear-sky upwelling brightness temperature spectra recorded on 19 April 2007. (Lower panel) residual differences (observed – calculated GENLN2 spectrum) for both Met Office and ECMWF upper atmosphere fields, see legend.

To gauge the improvement over the assumption of a spectrally constant emissivity, Figure 11 compares simulations including a fixed emissivity of 0.98. Whereas with a retrieved spectral emissivity the residuals are generally within ± 0.5 K, with a (higher) fixed emissivity there is a bias of approximately -1 K across the spectrum. This shows the importance of including a realistic surface emissivity in the forward modelling of IASI spectra over land.

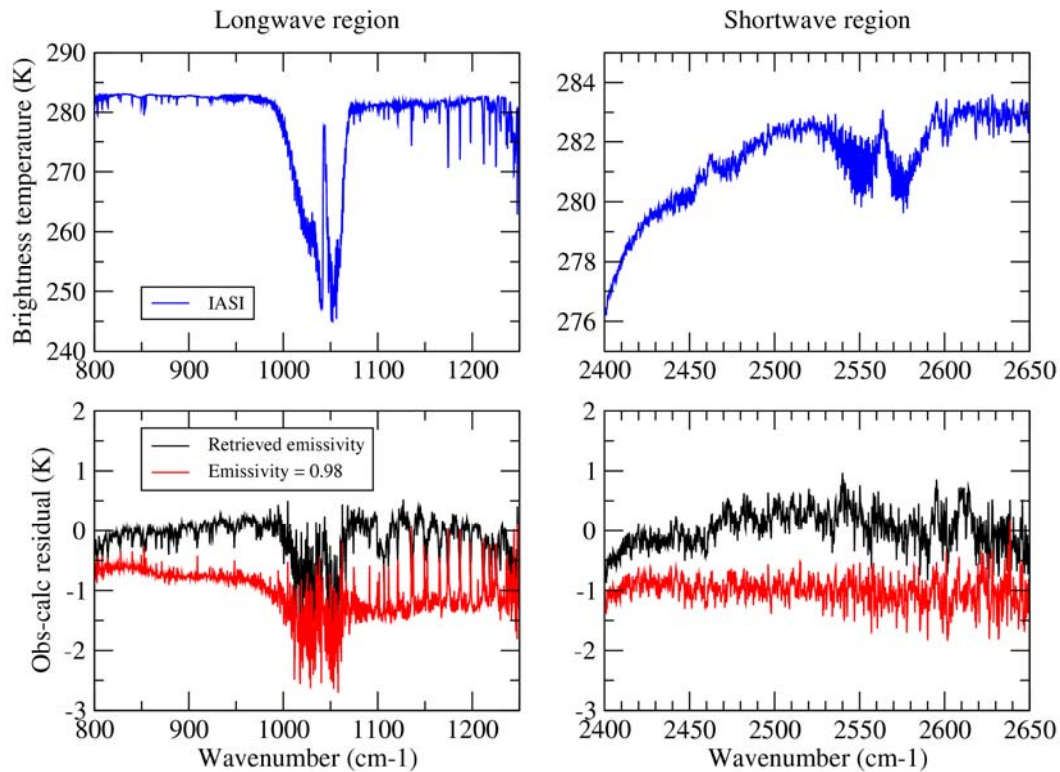


Figure 11: Comparison of simulations with differing surface emissivity assumptions. The upper panels show the average IASI brightness temperature over longwave and shortwave spectral regions. The lower panels show obs – calc residuals, using both ARIES retrieved and fixed (0.98) emissivity values.

5. Gulf of Mexico case study 29 April 2007

The final case study discussed here concerns a coordinated BAe 146 and WB-57 flight on 29 April 2007, conducted over the Gulf of Mexico with a MetOp overpass at 1550 UTC. This case study is particularly advantageous for studying instrument inter-calibrations because all four interferometers on the FAAM BAe 146, WB-57 and MetOp were operational on this day. Figure 12 shows that the northern portion of the flight track was clear of cloud, and again the case study instrument FOVs have been confined to this geographic area. Figure 13 shows the measurement collocations in more detail. Dropsondes were launched in close proximity to the overpass time (1531 and 1540 UTC).

Since the two aircraft and MetOp operate at different altitudes, their respective interferometers are sensitive to different parts of the atmosphere, at least over those spectral regions with transmittances significantly less than unity. However, in microwindows in the 800-1200 cm^{-1} region the upwelling radiances are dominated by surface emission and the water vapour self-broadened continuum which is overwhelmingly dependent on the concentration of lower-tropospheric water vapour. Hence, it is possible to compare directly radiances from the four instruments to test their respective calibration accuracies. Note that the satellite zenith angle for the IASI footprints does not exceed 2.6° for the selected FOVs, so it is legitimate to compare these data with directly upwelling radiances recorded by the other interferometers.

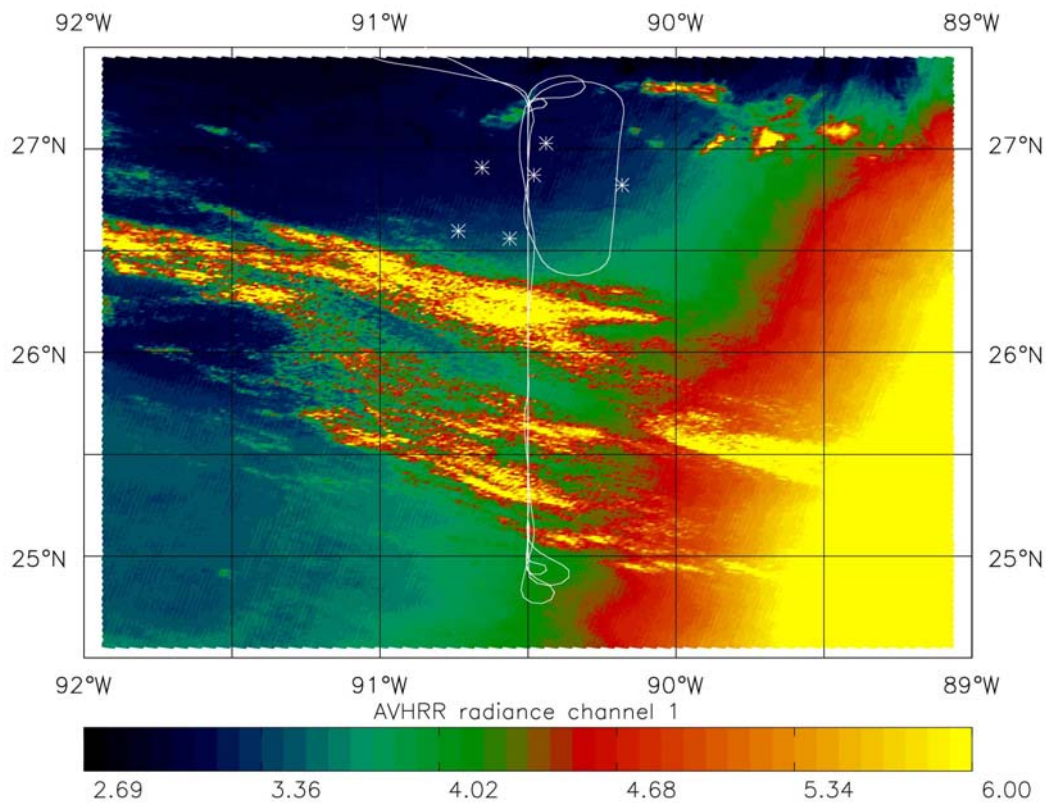


Figure 12: MetOp AVHRR channel 1 image (580-680 nm) overlaid with FAAM BAe 146 flight track and (white asterisks) selected clear IASI FOVs. The brightest parts of the AVHRR image show the presence of clouds due to solar reflection. Note that sun glint contaminates this image.

Figure 14 compares the average brightness temperatures for IASI, NAST-I, S-HIS and ARIES. Their respective sensitivity to progressively warmer parts of the atmosphere is seen in the trend of brightness temperatures, e.g. below 700 cm^{-1} in the longwave CO_2 band. However, all instruments record very similar brightness temperatures in parts of the atmospheric window region. Figure 15 shows the same information, but expanded in a small part of the window region; also an apodisation function has been applied to the spectra to standardise their effective spectral resolutions and aid direct comparison. In microwindows insensitive to the upper atmosphere the level of agreement between all four instruments is striking, with only 0.3 K separating these independent measurements. Thus, it can be claimed with confidence that the radiometric accuracy of IASI is within 0.3 K, a statement that is corroborated by results from the other case studies (see Figure 3).

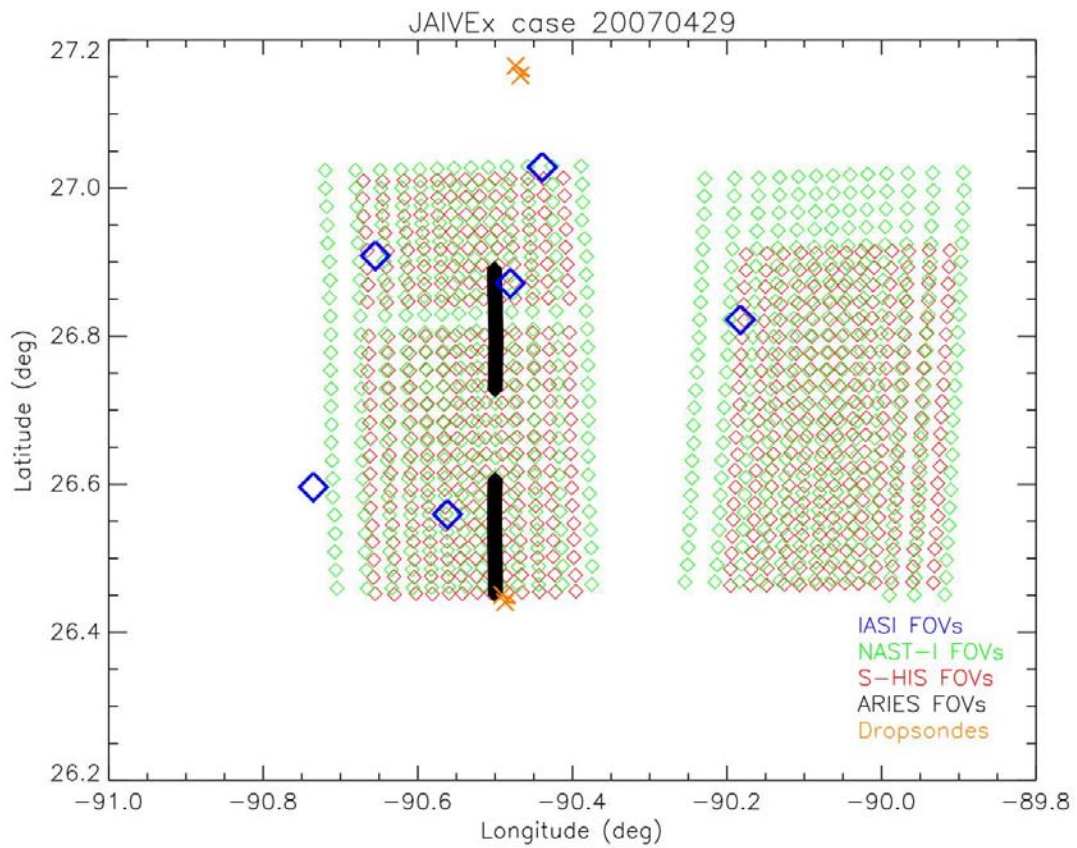


Figure 13: Collocation of observations on 29 April 2007. The diamond symbols denote (the centres of) individual instrument footprints on the ground, while crosses show the launch and terminating coordinates of dropsondes, see legend.

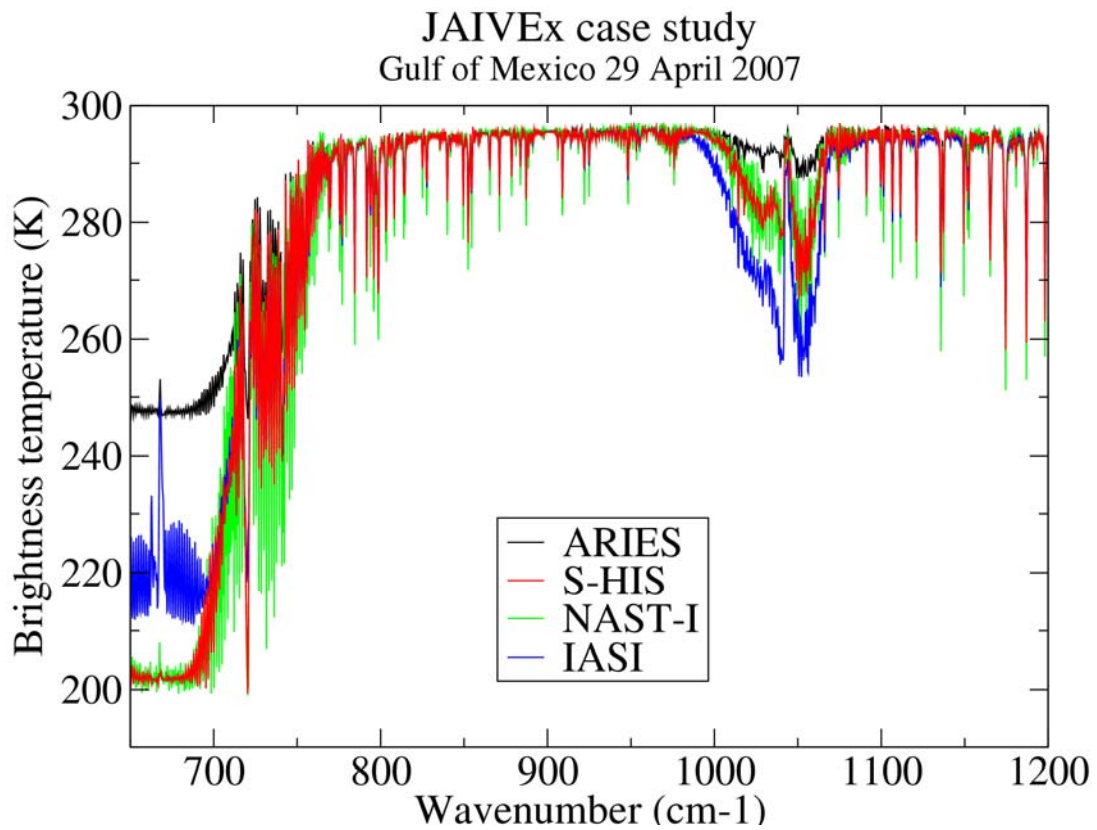


Figure 14: Comparison of average brightness temperatures from four interferometers, measured on 29 April 2007.

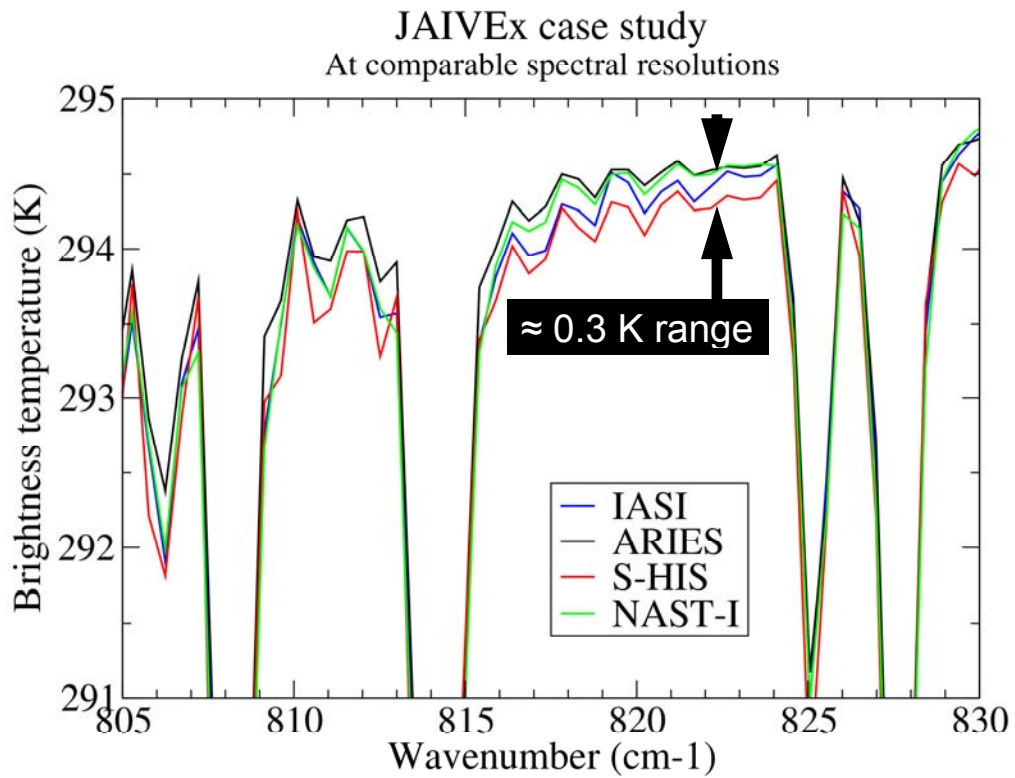


Figure 15: As Figure 14, but over a reduced spectral range.

6. Summary

The JAIVEX campaign, bringing together hyperspectral radiance measurements with high-density collocated observations of the atmospheric state, has produced a valuable dataset for validation of satellite calibration accuracy and retrieval algorithms.

Three case studies described here have been used to test the absolute calibration accuracy of IASI. Line-by-line simulations of radiances measured over ocean match the observations to within 0.2 K over the 800-1200 cm^{-1} region, and within 1.0 K over much of the rest of the spectrum. Allied with agreement of four independent interferometer measurements to within 0.3 K, it can be concluded that the calibration accuracy of IASI is, at worst, a few tenths of a degree. The importance of constraining the surface emissivity and temperature characteristics is demonstrated for IASI data over land.

The JAIVEX dataset is freely available for academic research, contact stu.newman@metoffice.gov.uk for more information.

Acknowledgements

This work has been partially funded under EUMETSAT contract Eum/CO/06/1596/PS. The FAAM BAe 146 is jointly funded by the Met Office and the Natural Environment Research Council. The US team was sponsored by the National Polar-orbiting Operational Environmental Satellite System (NPOESS) Integrated Program Office (IPO) and NASA.

References

- Edwards, D. P., 1992: GENLN2: A general line-by-line atmospheric transmittance and radiance model, *NCAR Tech. Note NCAR/TN-367+STR*, National Center for Atmospheric Research, Boulder, Co., USA.
- Clough, S. A., M. W. Shephard, E. J. Mlawer, J. S. Delamere, M. J. Iacono, K. Cady-Pereira, S. Boukabara, and P. D. Brown, 2005: Atmospheric radiative transfer modeling: a summary of the AER codes, Short Communication, *J. Quant. Spectrosc. Radiat. Transfer*, *91*, 233-244
- Newman, S. M., Smith J. A., Glew M. D., et al., 2005: Temperature and salinity dependence of sea surface emissivity in the thermal infrared, *Quart. J. Royal Meteorol. Soc.* *131* (610), 2539-2557
- Newman, S. M., F. Hilton, S. Clough and A. D. Collard, 2008: Identification of biases in the modelling of high peaking water vapour channels from IASI, *Proceedings of ITSC-XVI, Angra dos Reis, Brazil, 7th-13th May 2008*
- Taylor, J. P., W. Smith, V. Cuomo et al., 2008: EAQUATE – An International Experiment For Hyper-spectral Atmospheric Sounding Validation, *Bull. Am. Meteorol. Soc.*, *89*, 203-218
- Tobin, D. C., Revercomb H. E., Knuteson R. O., et al., 2006: Radiometric and spectral validation of Atmospheric Infrared Sounder observations with the aircraft-based Scanning High-Resolution Interferometer Sounder, *J. Geophys. Res.*, *111* (D9), D09S02